JOURNAL OF Applied Polymer SCIENCE

Special Issue: Manufacturing of Advanced Biodegradable Polymeric Components

Guest Editors: Prof. Roberto Pantani (University of Salerno) and
Prof. Lih-Sheng Turng (University of Wisconsin–Madison)

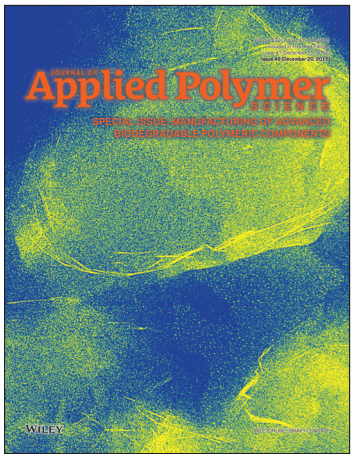

EDITORIAL

REVIEWS

ARTICLES

JOURNAL OF Applied Polymer SCIENCE

Special Issue: Manufacturing of Advanced Biodegradable Polymeric Components

Guest Editors: Prof. Roberto Pantani (University of Salerno) and Prof. Lih-Sheng Turng (University of Wisconsin–Madison)

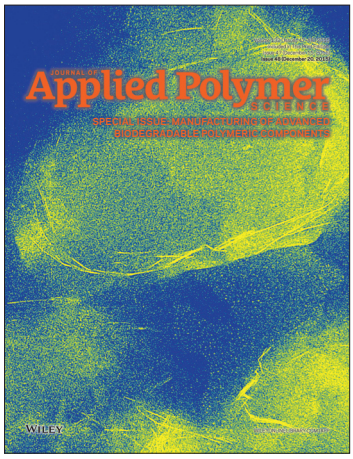

Rotational molding of biodegradable composites obtained with PLA reinforced by the wooden backbone of opuntia ficus indica cladodes
A. Greco and A. Maffezzoli, *J. Appl. Polym. Sci.* 2015, **DOI:** 10.1002/app.42447

Foam injection molding of poly(lactic) acid: Effect of back pressure on morphology and mechanical properties
V. Volpe and R. Pantani, *J. Appl. Polym. Sci.* 2015, **DOI:** 10.1002/app.42612

Modification and extrusion coating of polylactic acid films
H.-Y. Cheng, Y.-J. Yang, S.-C. Li, J.-Y. Hong and G.-W. Jang, *J. Appl. Polym. Sci.* 2015, **DOI:** 10.1002/app.42472

Processing and properties of biodegradable compounds based on aliphatic polyesters
M. R. Nobile, P. Cerruti, M. Malinconico and R. Pantani, *J. Appl. Polym. Sci.* 2015, **DOI:** 10.1002/app.42481

Journal of Applied Polymer Science

Biorenewable polymer composites from tall oil-based polyamide and lignin-cellulose fiber

Kunwei Liu,[1] Samy A. Madbouly,[1,2] James A. Schrader,[3] Michael R. Kessler,[4] David Grewell,[5] William R. Graves[3]

[1]Department of Materials Science and Engineering, Iowa State University, Ames, Iowa
[2]Department of Chemistry, Faculty of Science, Cairo University, Orman-Giza, Egypt
[3]Department of Horticulture, Iowa State University, Ames, Iowa
[4]School of Mechanical and Materials Engineering, Washington State University, Pullman, Washington, D.C.
[5]Department of Agriculture and Biosystems Engineering, Iowa State University, Ames, Iowa
Correspondence to: S. A. Madbouly (E-mail: madbouly@iastate.edu)

ABSTRACT: Tall oil-based polyamide (PA) was blended with lignin-cellulose fiber (LCF), an inexpensive, highly abundant byproduct of the pulp and paper industries, to produce environmental-friendly thermoplastic biocomposites. The effects of the concentration of LCF on the thermal, rheological, and mechanical properties of the composites were studied using differential scanning calorimetry (DSC), dynamic mechanical analysis (DMA), thermogravimetric analysis (TGA), rheological testing, and mechanical testing. The morphologies of the composites were investigated using scanning electron microscopy (SEM). The incorporation of LCF did not change the glass relaxation process of the polyamide significantly. Results from rheological testing showed that the complex viscosity and shear storage modulus were increased by LCF. Both the modulus and strength increased with increasing LCF content; however, LCF substantially reduced the tensile elongation of the composites. The thermal stability of the composites was strongly influenced by the concentration of LCF. The onset of the degradation process shifted to lower temperatures with increasing LCF content. We conclude that LCF has strong potential for use as filler that is compatible with tall oil-based polyamide. Adding LCF to form PA-LCF composites can lower material costs, reduce material weight, and increase strength and rigidity compared to neat PA. Composites of PA-LCF could serve as sustainable replacements for petroleum plastics in many industrial applications and would provide additional opportunities to utilize LCF, a highly abundant biorenewable material. © 2015 Wiley Periodicals, Inc. J. Appl. Polym. Sci. **2015**, *132*, 42592.

KEYWORDS: biomaterials; biopolymers and renewable polymers; blends; composites; differential scanning calorimetry (DSC)

Received 5 April 2015; accepted 2 June 2015
DOI: 10.1002/app.42592

INTRODUCTION

Polymers and composites derived from biorenewable resources have received extensive attention as sustainable alternatives to petroleum-based polymers due to the increasing cost of fossil resources and growing environmental concerns. It is estimated that economically viable petroleum supplies will be depleted within 100 years.[1] Biorenewable resources are generally defined as organic materials of recent biological origin.[2] Traditional petroleum-based polymers are sourced from nonrenewable carbon, and most of them are not biodegradable. The wide use of petroleum-based polymers has introduced many environmental problems, such as increased greenhouse gas emissions, white pollution, and a large and growing burden on solid-waste disposal systems. Replacement of petroleum-based materials with bio-based materials for disposable plastic products has the potential to reduce both solid waste (if the new bio-based product is biodegradable) and atmospheric carbon dioxide (the carbon in all biobased materials originates by the uptake of carbon dioxide from the atmosphere by plants). Biorenewable materials are carbon neutral if they end their life cycle through biodegradation, because the carbon dioxide originally taken up by plants is returned to the atmosphere. If landfilled at the end of their life cycle, biorenewable materials would be carbon negative. The carbon dioxide originally fixed by plants would be sequestered in the landfill.

Many thermoplastics and thermosets based on biorenewable resources have been developed. Polylactide (PLA) is a widely used thermoplastic produced from the fermentation of corn and sugar feedstocks. Because PLA is biorenewable and biodegradable, it has been used in packaging and biomedical applications.[3,4] Another carbohydrate-based bioplastic, polyhydroxyalkanoates (PHA), is a class of polyesters produced by bacteria for carbon

and energy storage.[5] PHA is biorenewable and biodegradable, and it also possesses high biocompatibility. PHA materials have been used as drug carriers and scaffold materials in tissue engineering.[6–8] PHA possesses mechanical properties similar to those of polypropylene; however, the high cost and the brittleness of PHA have limited its application as a general plastic.

Plant oils, such as soybean oil, castor oil, and tung oil, are very popular starting materials for synthesizing biorenewable thermoplastics and thermosets because they possess many chemical reactive sites such as double bonds, hydroxyl groups, epoxide groups, and ester linkages. Polyamide (PA) is a class of polymer that has been widely used in textiles, automotive, electrical, and adhesive applications.[9] Although some of the most highly utilized polyamides are produced from petroleum-based chemicals, industrial polyamides have also been synthesized from vegetable oils. Polyamide-11, a castor oil-based polyamide produced by Arkema, can be synthesized via polycondensation of 11-aminoundecanoic acid (a fatty acid derived from castor oil).[10] Another way to synthesize biorenewable polyamide involves the use of a vegetable oil-based dimer. Plant oils are first saponified into fatty acids and then converted to dimer acid.[11] Hablot *et al.* synthesized polyamide based on rapeseed oil dimer acid and 1,2-diaminoehtane, 1,6-diaminohexane or 1,8-diaminooctaine.[12] The polyamides produced by this method are semi-crystalline polymers with a degree of crystallinity around 10%. The melting points of polyamides range from 79°C to 105°C, and the glass transition temperatures (T_g) range from −17°C to −5°C.[12] Polyamides are typically soft and flexible with maximum tensile strain of over 300%. Fan *et al.* prepared a series of polyamides using soy-based dimer acids with glass transition temperatures as high as 63°C and a modulus values above 2000 MPa.[13] Polyamides from tung oil, soybean oil, and tall oil have been widely utilized by the paint industry due to their thixotropic rheological properties.[14]

Although most biorenewable polymers are considered to be more sustainable and environmentally friendly than petroleum-based polymers, they are generally more expensive, and most do not match the mechanical properties offered by comparable petroleum plastics. At their present stage of industrial development, PLA and PHA are more expensive than common petroleum-based polymers such as polyethylene and polystyrene, and they are inherently more brittle. A common approach used to decrease the overall cost and modify the mechanical properties of biorenewable polymers is to blend them with fillers or fibers. Plant-based fibers such as kenaf, jute, and bamboo, and synthetic fibers such as glass and carbon have been added to PLA to improve mechanical properties.[15–19] Generally, the strength and modulus are both increased by adding rigid fibers into the PLA matrix if strong interfacial adhesion can be achieved. Moreover, adding agriculture-based fillers can increase the biodegradation rate of the biodegradable polymers. For example, adding distiller dried grains (DDGS), a cereal co-product of the corn-ethanol industry, into PHA not only decreases the overall cost of the composites, but also increases the biodegradation rate significantly.[19,20] The effects of organic fillers such as flours, starches, rice straw, lignin, and cellulose have been examined for many biorenewable thermoplastics,[21–26] but no research has been published that examines the effects of blending lignin-cellulose fiber (LCF) with tall oil-based polyamide.

Lignin is the second most abundant plant-derived resource next to cellulose,[20,21] and it is a byproduct of the paper, pulp, and bio-ethanol industries.[22,23] Lignin is an amorphous low-molecular-weight polymer produced in plants by dehydrogenative polymerization of three types of phenols: p-coumaryl, coniferyl, and sinapyl alcohols.[24,25] In woody plants, lignin offers protection against water, pathogens, pests, and enzymatic degradation.[20,24] Lignin also acts as a binder that holds hemicellulose and cellulose together, providing stiffness to a plant.[26] Because of its complex structure, it is one of the most persistent natural organic molecules, and it is a very important component of organic soils. Lignin has been used as filler for many thermoplastics. The incorporation of lignin can alter the mechanical properties, thermal stability, and crystallization behavior of the thermoplastics.[27–29] Cellulose is a polysaccharide consisting of D-glucose linked by β-1,4 linkage.[30] It forms the primary structural component in plants. Cellulose is a hydrophilic, biodegradable, and semi-crystalline polymer.[31,32] Blending plant-based fillers such as cellulose and lignin with biorenewable plastics can increase strength, modify biodegradability, and reduce costs compared to that of the base polymer.

The objective of this study was to characterize the thermal, mechanical, rheological, and morphological properties of a tall oil-based polyamide reinforced with LCF at three weight percentages and to compare the character of the three composites to each other and to pure PA. The fracture surface morphology was studied using scanning electron microscopy (SEM). Dynamic mechanical analysis (DMA) and differential scanning calorimetry (DSC) were performed to study the thermomechanical properties of the PA-LCF composite. Thermogravimetric analysis (TGA) was used to investigate the effect of LCF on the thermal stability of the PA-based material, and the rheological behavior of the composites was studied using a rheometer. Standard dog-bone shaped specimens for tensile testing were prepared to investigate the change in yield strength, modulus, and elongation after incorporating LCF into the tall oil-based polyamide. This research reports for the first time the composition and properties of blended PA-LCF and will provide engineers and designers with practical data for evaluating the performance and industrial potential of these novel composites.

EXPERIMENTAL

Materials

The polyamide (PA) used in this study was UNI-REZ™ 2651 supplied by Arizona Chemical, Jacksonville, FL. This polyamide is produced from fatty-acid dimers of tall oil, a compound extracted from pine tree as a byproduct of paper and wood pulp production. The specific chemical identity and percentage of composition of the tall oil-based polyamide used in our study are proprietary and have not been disclosed. UNI-REZ™ 2651 polyamide is highly flexible, with a maximum elongation of over 500%. It has a softening point between 95°C and 105°C and an amine value of five. The lignin-cellulose fiber (LCF) used in this study was Neroplast®, a filler obtained from New

Polymer Systems (New Canaan, CT) in 100-mesh powder form. Neroplast® is produced from virgin and uncontaminated lignocellulose sources such as pine trees. The Neroplast® filler contains a mixture of cellulose and lignin. The hemicellulose in the original lignocellulose sources was thermally and chemically removed to improve water resistance (hydrophobicity).

Composite Preparation

Before compounding, PA and LCF were dried at 60°C for 24 h to remove moisture. All the composites were prepared by compounding PA with the selected weight percentages of LCF using a twin-screw micro-compounder (DACA Instrument, Santa Barbara, CA). Compounding was performed at a rotational speed of 100 rpm for 10 min. The temperature of the barrel was set to 140°C. The neat PA polymer was also processed using the same conditions so that the samples had the same thermal history. Composites with LCF at three selected weight percentages (10 wt %, 20 wt %, and 30 wt %) were prepared. The nomenclature for the composites in this study is presented with the base resin (polyamide) indicated with the letters PA, and the percentage of LCF filler shown numerically, for example, PA-20% represents the composite containing 20 wt % of LCF and 80 wt % of PA. After compounding, the extruded blends were compression molded using a Carver Model 4394 hydraulic press (Wabash, IN) to form DMA and tensile-testing specimens. The temperature for compression molding was set to 140°C. The compression force was set to 20,000 N (or 1.4 MPa in terms of pressure). The specimens were cooled to room temperature under pressure before being taken out of the mold.

Morphological Characterization

Samples of the composites and the base polymer were cryogenically fractured and viewed under an FEI Quanta FEG 250 scanning electron microscope (SEM) to examine and compare their morphologies. Before the samples were put into the SEM, they were sputter coated with a 5 nm-thick layer of iridium. The SEM images were taken at a working voltage of 10 kV under high vacuum.

Optical Microscopy

In order to observe the original shape of the LCF particles before compounding, LCF was dispersed in water and the mixture was placed between two parallel glass plates. The sample was then observed by using an Olympus BX-51 optical microscope.

DMA Measurements

DMA was performed using a Q800 dynamic mechanical analyzer from TA Instruments (New Castle, DE). Rectangular specimens with a dimension of 30 mm × 12.5 mm × 1.9 mm from compression molding were used for the DMA measurements. DMA was run in three-point bending mode over the temperature range from −100°C-90°C with a heating rate of 3°C/min, a frequency of 1 Hz, and a displacement amplitude of 20 μm. The storage modulus (E′) and the tan δ were recorded as a function of temperature.

DSC Measurements

Differential scanning calorimetry (DSC) analysis were performed by using a TA Instruments Q20 differential scanning calorimeter. All DSC measurements were carried out in a nitrogen atmosphere. The heating and cooling rates for the DSC experiment were set to 30°C/min. A sample weight of 15 to 20 mg was used. Calibration on the DSC machine was performed using an indium sample prior to the experiment. To erase the thermal history, samples were heated from room temperature to 150°C. The molten samples were then cooled to −100°C and heated again to 150°C. The second heating run (with no previous thermal history due to processing) was used to study the thermal properties of the PA-LCF composites.

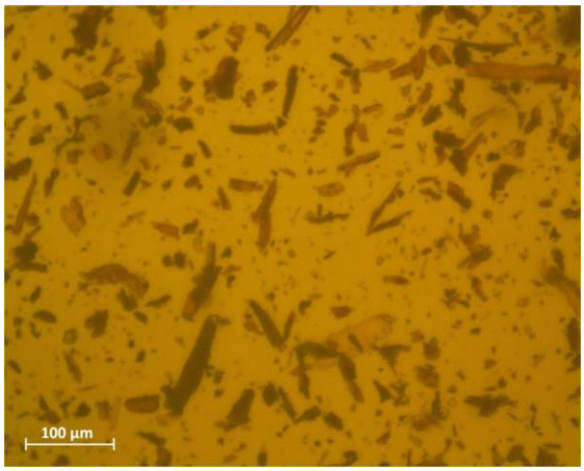

Figure 1. Optical micrograph of LCF. [Color figure can be viewed in the online issue, which is available at wileyonlinelibrary.com.]

TGA Measurements

TGA was carried out using a Q50 thermogravimetric analyzer from TA Instruments. Samples weighing approximately 5 mg were heated from 25°C to 800°C under a nitrogen atmosphere at a heating rate of 20°C/min.

Rheological Measurements

The rheological properties of the PA and PA-LCF composites were studied using an AR2000ex rheometer (TA Instruments). Frequency sweeps with 5% strain from 0.1 rad/s and 100 rad/s were performed. The diameter of the plates was 25 mm, and the gap between the plates was set to between 0.5 mm to 0.6 mm. The storage modulus and complex viscosity as a function of angular frequency were evaluated.

Mechanical Testing

The tensile properties of the samples (five samples for each blend composition) were determined according to ASTM D638 guidelines by using an Instron 5569 universal testing machine. A load cell with 5 kN capacity was utilized. The tensile testing was conducted at room temperature with a crosshead speed of 50 mm/min. The mechanical properties of each composition were determined by averaging the data for the five samples. The Young's modulus, yield strength, and strain at break were analyzed as a function of LCF content.

RESULTS AND DISCUSSION

Optical Microscopy and SEM

The LCF is a black substance in its original, purchased form. An optical micrograph illustrating the shape and size of the

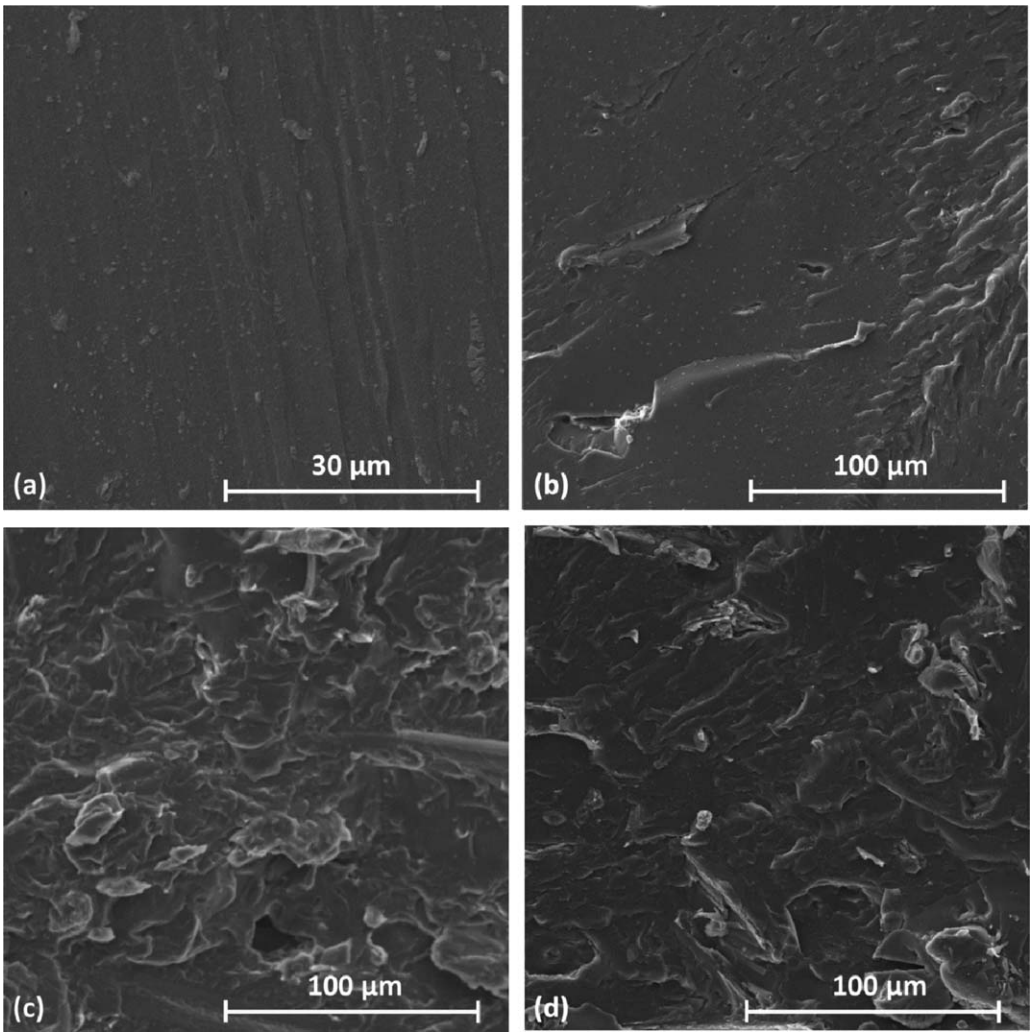

Figure 2. SEM images of the fracture surfaces of (a) PA-0%; (b) PA-10%; (c) PA-20%; and (d) PA-30%.

LCF particles is shown in Figure 1. Most of the LCF was in fiber form, but globular form was also observed. The length of the fiber used in this study ranged from 20 µm to 100 µm.

The morphology of the PA/LCF biocomposites was investigated using an SEM. Figure 2 shows the cryogenic fracture surface of all prepared compositions. The pure PA polymer shown in Figure 2(a) is almost featureless except for some loose polymers resting on top of the surface due to fracture. In Figure 2(b), it is evident that the LCF is wetted in the matrix. There are several cavities on the fracture surface, indicating that LCF have been pulled out from the matrix. Figure 2(c,d) show that the LCF is homogeneously distributed in the matrix. In addition, there is no gap or cavity between the LCF and the polymer matrix, and very few voids are observed, indicating a good interfacial adhesion between the LCF and the matrix.

Rheology

In order to investigate the effect of LCF incorporation on the rheological properties of PA-based composites, samples were tested with a rheometer using a frequency sweep at 140°C. Figure 3 depicts the change of shear storage modulus in relation to angular frequency and shows that the modulus of all samples increased with increasing angular frequency. It is also apparent that an increase in LCF content increased the shear storage modulus across the entire frequency range, a behavior consistent with the notion that incorporation of rigid fillers restricts deformation of polymers. For comparison, the storage modulus of PA-30% at 0.1 rad/s is about 5.3 times higher than that of pure PA polymer.

Figure 4 shows the evolution of complex viscosity of PA polymer and the PA-LCF composites as a function of angular frequency. The complex viscosity of all samples decreased with increasing angular frequency; thus, the PA polymer and the composites all exhibited shear-thinning behavior, i.e., the material became less resistant to flow as the rate of shear stress increased. This shear-thinning behavior has often been observed in polymers containing filler particles.[33–35] As seen with the storage modulus results, the complex viscosity of PA-based

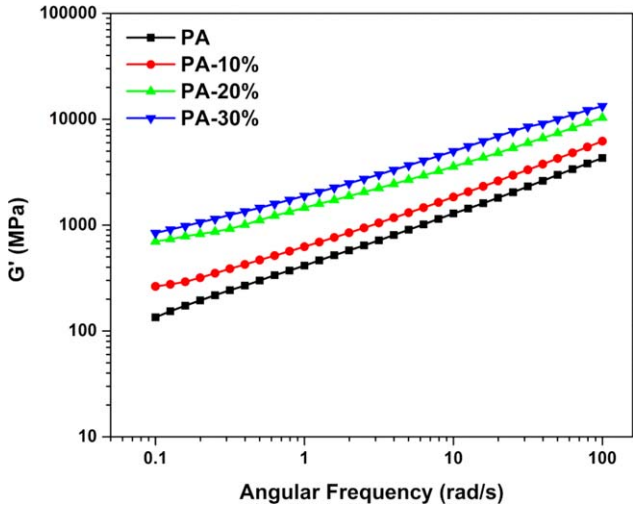

Figure 3. Angular frequency dependence of storage modulus at 140°C for PA-LCF composites containing different percentages of filler. [Color figure can be viewed in the online issue, which is available at wileyonlinelibrary.com.]

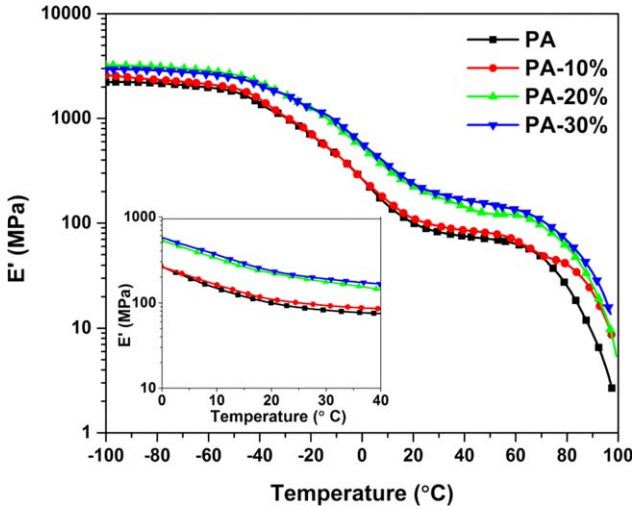

Figure 5. Storage modulus as a function of temperature for the pure PA polymers and its composites with 10 wt % to 30 wt % LCF. [Color figure can be viewed in the online issue, which is available at wileyonlinelibrary.com.]

composites increased with increasing LCF percentage, a phenomenon related to the decrease in mobility of the polymer chains as a result of the rigid LCF filler in the matrix.

Dynamic Mechanical Analysis (DMA)

The effects of LCF filler content on the storage modulus and the tan δ of the PA-LCF composites were examined by DMA over a temperature range from −100°C to 100°C (Figure 5). At −100°C (glassy region), the storage modulus of the PA polymer was greatly improved by the addition of LCF. The storage modulus of the composites reached the maximum with 20 wt % LCF content. The PA-30 wt % sample showed a lower storage modulus at −100°C compared to the composite with 20 wt % LCF, but it had a higher storage modulus than the PA-10% sample, indicating that, for the percentage LCF contents evaluated in our study, the reinforcement effect of LCF in the PA matrix reached its maximum at 20 wt % LCF at the glassy region. When the temperature increased to above −50°C, the PA underwent a glass-transition relaxation process, and a substantial decrease in storage modulus is evident. At temperatures above 60°C, the storage modulus decreased substantially again due to the softening of PA at high temperature. At room temperature, the storage modulus increased significantly with increasing percentage of LCF filler. For example, the storage modulus of pure PA polymer at room temperature was approximately 90 MPa, while the composite with 30 wt % LCF exhibited a modulus of approximately 210 MPa; therefore, a 133% increase in storage modulus was observed after adding 30 wt % of LCF. The increase in modulus is ascribed to the reinforcement effect of the LCF fiber in the soft PA matrix.

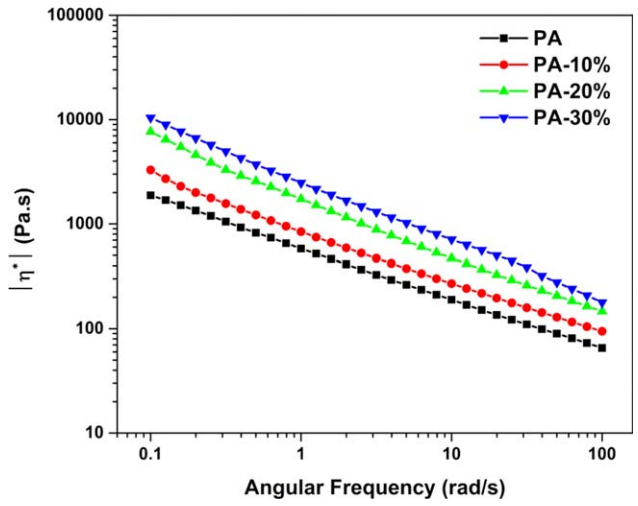

Figure 4. Angular frequency dependence of complex viscosity at 140°C for PA-LCF composites containing different percentages of filler. [Color figure can be viewed in the online issue, which is available at wileyonlinelibrary.com.]

The tan δ curves of pure PA and the PA-LCF composites are shown in Figure 6. The broad tan δ peak in the range of −20°C to 50°C is associated with the glass transition process (α-relaxation process) of the PA. The glass transition process indicates the rapid increase of the sliding movement of the amorphous polymeric chains in PA due to high temperatures. The temperature corresponding to the maxima of the tan δ is generally considered the glass transition temperature (T_g). The glass transition temperature of all prepared composites ranged from 5.7°C to 7.2°C. It is clear that the concentration of LCF has little effect on the glass transition temperature of the composites. The PA-30% composite showed an increase in the glass transition temperature of only a 1.5°C compared to pure PA polymer. In addition, the tan δ curves of all composites exhibited a shoulder at approximately −40°C. The shoulders were located at a constant temperature regardless of LCF content. The shoulder at this temperature is ascribed to the β-relaxation of the polyamide matrix. β-relaxation is caused by the rotational movement of the side groups and some loosely packed chain segments of PA.[36] The area under the tan δ curve of pure PA is

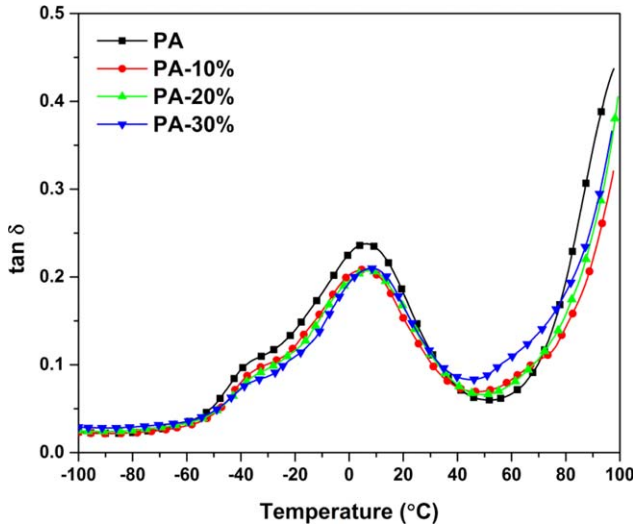

Figure 6. Tan δ curves as a function of temperature obtained via DMA. [Color figure can be viewed in the online issue, which is available at wileyonlinelibrary.com.]

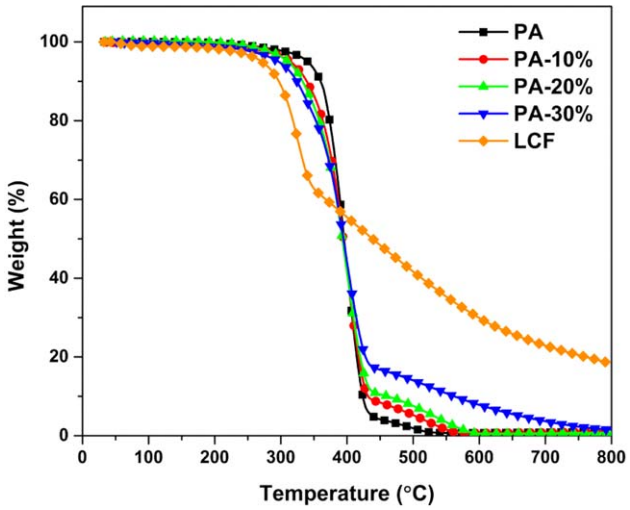

Figure 8. Thermal degradation behavior of pure PA polymer, pure LCF, and PA-LCF composites. [Color figure can be viewed in the online issue, which is available at wileyonlinelibrary.com.]

larger than those of PA/LCF composites, indicating that the damping ability of the composites is less than that of pure PA. This is also expected because adding rigid LCF into the soft PA matrix decreased the mobility of PA polymeric chain.

Differential Scanning Calorimetry (DSC)

DSC was performed to study the effect of LCF filler content on the thermal behavior of PA-LCF composites, particularly the melting point and glass transition temperature. Figure 7 shows the DSC traces of pure PA polymer and PA-LCF composites during the second heating run (after all the thermal history had been removed). For pure PA and the composites, there was a very broad glass transition from −56°C to −10°C. The glass transition temperature was approximately 33°C, regardless of filler content. There was an endothermic peak between 80°C and 90°C that is associated with the melting of the crystalline region in the PA polymer. The location of melting peaks shifted slightly to higher temperatures as the content of LCF increased, indicating that the LCF may act as a crystallization nucleating agent for PA polymer. Lignin-based filler was found to be a good nucleating agent for various semi-crystalline polymers.[29,37]

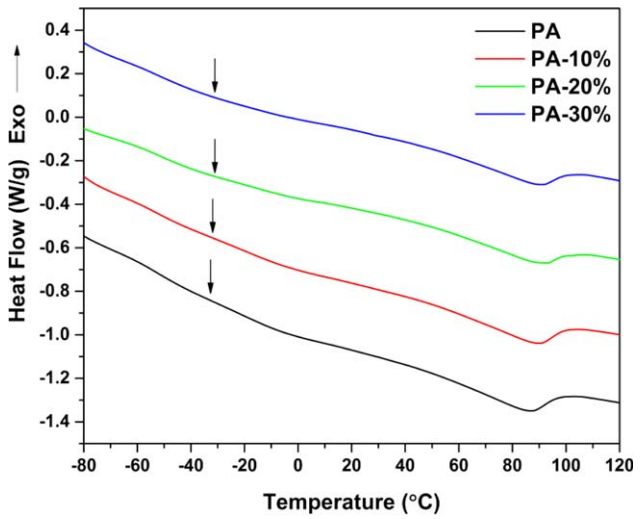

Figure 7. DSC traces of PA polymer and composites containing 10, 20, and 30 wt % of LCF. [Color figure can be viewed in the online issue, which is available at wileyonlinelibrary.com.]

Thermogravimetric Analysis (TGA)

The thermal degradation behaviors of the PA-LCF composites were studied using TGA. Figure 8 shows the TGA measurements for pure PA, pure LCF, and the three PA-LCF composites. PA polymer showed major thermal degradation beginning at approximately 355°C and had lost almost all its original mass at temperatures approaching 440°C. The pure LCF began to degrade at a temperature around 290°C, and the degradation rate of LCF decreased substantially when the temperature reached 345°C. Table I presents the temperature values corresponding to the 5% weight loss (T_5), the temperatures corresponding the 10% weight loss (T_{10}), the onset degradation temperature (T_{onset}), and the maximum degradation temperature of all samples (T_{max}). After comparing the thermal degradation behavior of composites with different content of LCF, it is clear that the onset-degradation temperature, T_5, and T_{10} values shifted to lower temperatures with increasing LCF content. This indicates that increasing LCF filler content decreases the thermal stability of the composites in the temperature range between 250°C and 400°C. Figure 9 shows an enlarged view at

Table I. Degradation Temperature Values Derived from TGA

Samples	T_5 (°C)	T_{10} (°C)	T_{onset} (°C)	T_{max} (°C)
PA	340	360	355	400
PA-10%	314	339	342	400
PA-20%	312	333	336	399
PA-30%	296	324	320	399
LCF	271	297	296	326

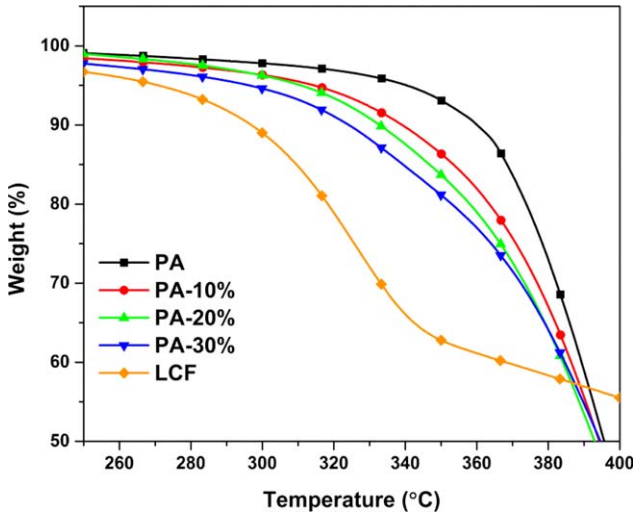

Figure 9. Enlarged portion of Figure 8 showing detail for the onset of thermal degradation. [Color figure can be viewed in the online issue, which is available at wileyonlinelibrary.com.]

the 250°C to 400°C region of Figure 8. The onset temperatures of thermal degradation for composites containing LCF at 0%, 10%, 20%, and 30% are 355°C, 342°C, 336°C, and 320°C, respectively. Due to the aromatic chemical structure of lignin, the thermal stability of the overall composites at temperatures between 400°C to 800°C was greatly increased with increasing LCF content (Figure 8).

Figure 10 illustrates the derivative rate of weight loss for all samples. The peaks in this figure indicate the temperature at which samples reached their maximum thermal degradation rate. Based on Figure 10, the largest peaks of the weight derivative curve for PA and PA-LCF composites are all at ≈400°C, regardless of the composition.

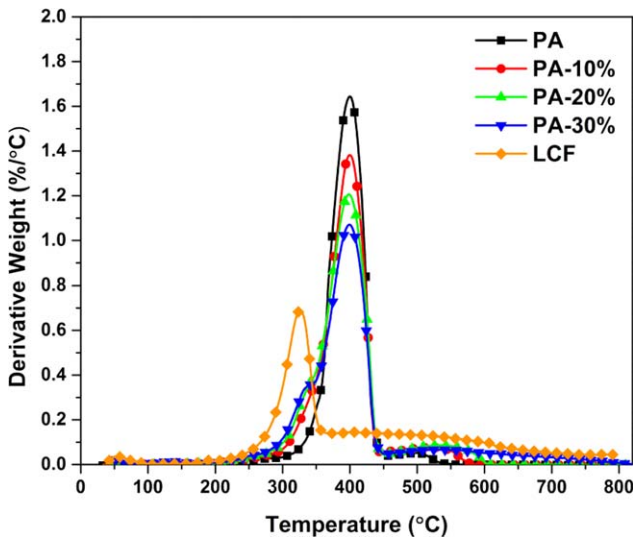

Figure 10. Weight derivative of pure PA polymer, LCF, and PA-LCF composites. [Color figure can be viewed in the online issue, which is available at wileyonlinelibrary.com.]

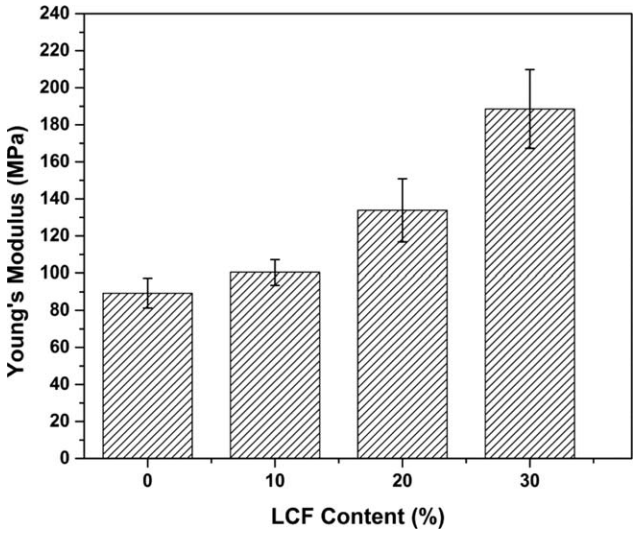

Figure 11. Young's modulus as a function of LCF content.

Mechanical Testing

Figures 11–13 show the mechanical properties (Young's modulus, yield strength, and strain at break, respectively) of pure PA (0% filler) and the PA-LCF composites with 10%, 20%, and 30% filler. Results revealed that the Young's modulus increased with increasing amount of LCF filler. The modulus value for the PA-30% composite was 188 MPa, while the modulus of pure PA polymer (0% LCF) was 90 MPa, showing that the modulus of PA-based materials can be doubled by adding 30 wt % LCF. Similar results have been found by Nitz *et al.*, who showed that blending lignin filler with polyamide-11 derived from castor oil can lead to a systematic increase in Young's modulus of the resulting composites; however, in their study, addition of 30 wt % lignin yielded only a ≈35% increase in modulus.[38] The yield strength of composites in our trial was compared as a function of LCF content (Figure 12). It is apparent that, within the range test (0% to 30% LCF), yield strength of PA-LCF composites increases with increasing LCF content.

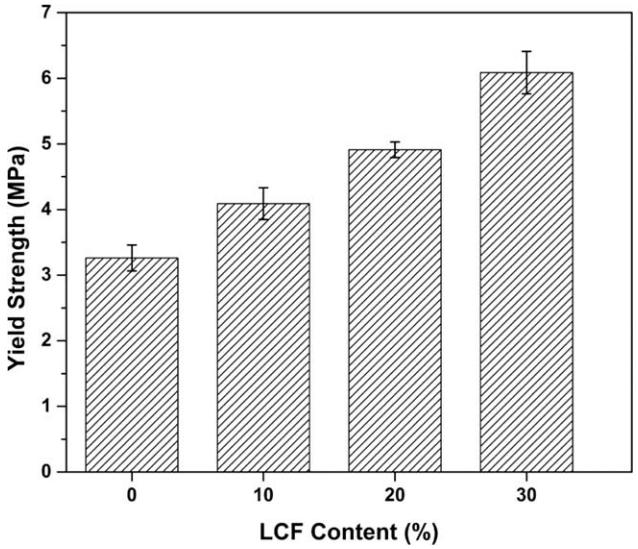

Figure 12. Yield strength as a function of LCF content.

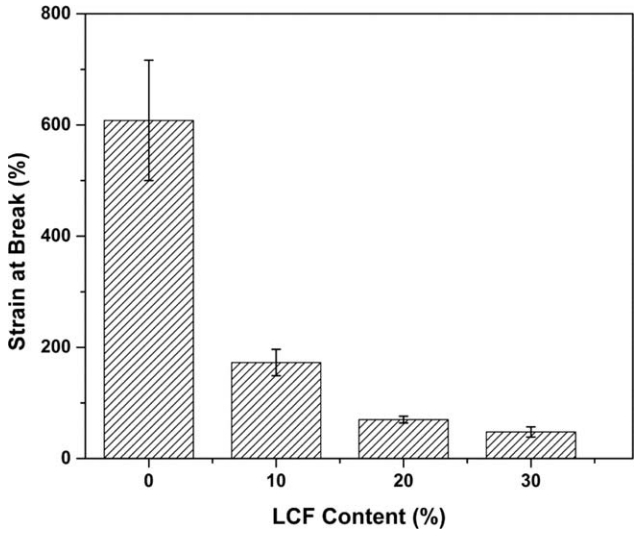

Figure 13. Strain at break as a function of LCF content.

The strength of the pure PA was about 3.3 MPa, compared to 6.1 MPa for the PA-30% composite. The increase of both Young's modulus and yield strength is likely attributed to the good dispersion of LCF and the good interfacial interaction between the filler and the PA matrix.[39]

The strain-at-break values for the composites are shown in Figure 13. The PA polymer was highly elastic and showed maximum strain at over 600% elongation. The strain at break decreased significantly with increasing LCF content. The most substantial reduction was observed with the increase of LCF content from 0% to 10%; the strain at break of the PA-10% composite decreased 70% compared to the pure PA polymer. For the PA-30% sample, the strain at break of the composite was only 47%. A substantial decrease in maximum strain is common in polymers blended with rigid fillers because filler particles decrease the mobility of the polymer chains when under an applied load. It is also common for the fillers to agglomerate in thermoplastic composites, a phenomenon that can further decrease the elongation elasticity of the material. Therefore, while the addition of LCF increases the modulus and strength of PA-based composites, it also makes the material more brittle.

Potential for Industrial Application

As a potential replacement for petroleum-based plastics, PA-LCF has many appealing characteristics. Like petroleum-based polypropylene, polyethylene, etc., PA-LCF can be injection molded, thermoformed, and formed into sheets and films. By varying the percentage of LCF composite material, the mechanical properties of the PA-LCF composite can be adjusted for specific applications (Figures 11–13). Compared to other common injection-moldable bioplastics, for example, PHA and PLA, which are somewhat brittle (Young's modulus of ≈1500 and ≈1960 MPa, respectively, and elongation at break of ≈4.6% and ≈5%, respectively), PA-LCF composites are more flexible and ductile (Young's modulus of ≈100 MPa and elongation at break of ≈190% for the PA-10% composite) and more closely resemble the mechanical properties of polypropylene and polyethylene (Young's modulus of ≈1500 and ≈200 MPa, respectively, and elongation at break of ≈ 150% and ≈ 400%, respectively).[31,32,40,41]

CONCLUSIONS

Tall oil-based polyamide was blended with lignin-cellulose fiber (a type of fiber that contains both cellulose and lignin) to produce environmental-friendly thermoplastic biocomposites. The effects of LCF on the thermal, mechanical, and rheological properties were investigated. DMA results indicated that the glass transition temperature of the PA-based material was only slightly affected by the addition of LCF filler. DMA results also showed that the storage modulus at room temperature increased with increasing amount of LCF. The increase in storage modulus indicates that a reinforcement effect is provided by the LCF fiber in the PA matrix. TGA tests were performed to characterize the thermal-degradation behavior of PA-LCF composites, and it was shown that incorporation of LCF filler decreased the thermal stability of the composites within the temperature range of 250°C to 400°C, but thermal stability of the composites was increased with increasing LCF content at temperatures between 400°C and 800°C. The dynamic viscosity and shear modulus increased significantly with increasing LCF filler content. Tensile testing was used to investigate the mechanical properties of the PA-LCF composites and showed that the Young's modulus and the yield strength increased with the additional of LCF filler, but that the strain at break was reduced. These results demonstrate that lignin-cellulose fiber can be blended with tall oil-based polyamides via melt processing to produce sustainable biorenewable composites that are affordable, possess useful mechanical properties, and can be easily adjusted to match specific industrial applications.

ACKNOWLEDGMENTS

This study was funded in part by the USDA Specialty Crops Research Initiative (NIFA-SCRI 2011-51181-30735) and by Iowa State University.

REFERENCES

1. Williams, C. K.; Hillmyer, M. A. *Polym. Rev.* **2008**, *48*, 1.
2. Brown, R. C.; Brown, T. R. Biorenewable Resources: Engineering New Products from Agriculture; John Wiley & Sons: Oxford, UK, **2013**.
3. Mills, C. A.; Navarro, M.; Engel, E.; Martinez, E.; Ginebra, M. P.; Planell, J.; Errachid, A.; Samitier, J. *J. Biomed. Mater. Res. A* **2006**, *76A*, 781.
4. Auras, R.; Harte, B.; Selke, S. *Macromol. Biosci.* **2004**, *4*, 835.
5. Zinn, M.; Witholt, B.; Egli, T. *Adv. Drug Deliver. Rev.* **2001**, *53*, 5.
6. Pouton, C. W.; Akhtar, S. *Adv. Drug Deliver. Rev.* **1996**, *18*, 133.
7. Sendil, D.; Gursel, I.; Wise, D. L.; Hasirci, V. *J. Control. Release* **1999**, *59*, 207.

8. Kassab, A. C.; Piskin, E.; Bilgic, S.; Denkbas, E. B.; Xu, K. *J. Bioact. Compat. Pol.* **1999**, *14*, 291.
9. Martino, L.; Basilissi, L.; Farina, H.; Ortenzi, M. A.; Zini, E.; Di Silvestro, G.; Scandola, M. *Eur. Polym. J.* **2014**, *59*, 69.
10. Karak, N. Vegetable Oil-Based Polymers Properties, Processing and Applications; Woodhead Publishing: Cambridge, UK; Philadelphia, **2012**.
11. Cavus, S.; Gurkaynak, M. A. *Polym. Adv. Technol.* **2006**, *17*, 30.
12. Kolb, N.; Winkler, M.; Syldatk, C.; Meier, M. A. R. *Eur. Polym. J.* **2014**, *51*, 159.
13. Fan, X. D.; Deng, Y. L.; Waterhouse, J.; Pfromm, P. *J. Appl. Polym. Sci.* **1998**, *68*, 305.
14. Oldring, P. K. T.; SITA Technology. Resins for Surface Coatings; Wiley: Chichester, New York, **2000**.
15. Tokoro, R.; Vu, D. M.; Okubo, K.; Tanaka, T.; Fujii, T.; Fujiura, T. *J. Mater. Sci.* **2008**, *43*, 775.
16. Huda, M. S.; Drzal, L. T.; Mohanty, A. K.; Misra, M. *Compos. Sci. Technol.* **2008**, *68*, 424.
17. Ma, H.; Joo, C. W. *J. Compos. Mater.* **2011**, *45*, 1451.
18. Ahmed, I.; Cronin, P. S.; Abou Neel, E. A.; Parsons, A. J.; Knowles, J. C.; Rudd, C. D. *J. Biomed. Mater. Res. B* **2009**, *89B*, 18.
19. Wan, Y. Z.; Wang, Y. L.; Li, Q. Y.; Dong, X. H. *J. Appl. Polym. Sci.* **2001**, *80*, 367.
20. Achyuthan, K. E.; Achyuthan, A. M.; Adams, P. D.; Dirk, S. M.; Harper, J. C.; Simmons, B. A.; Singh, A. K. *Molecules* **2010**, *15*, 8641.
21. Yang, H. P.; Yan, R.; Chen, H. P.; Zheng, C. G.; Lee, D. H.; Liang, D. T. *Energ. Fuel* **2006**, *20*, 388.
22. Solomon, B. D.; Barnes, J. R.; Halvorsen, K. E. *Biomass Bioenerg.* **2007**, *31*, 416.
23. Thielemans, W.; Wool, R. P. *Compos. Appl. Sci. Manuf.* **2004**, *35*, 327.
24. Laurichesse, S.; Averous, L. *Prog. Polym. Sci.* **2014**, *39*, 1266.
25. Mohanty, A. K.; Misra, M.; Drzal, L. T. *J. Polym. Environ.* **2002**, *10*, 19.
26. Boudet, A. M.; Kajita, S.; Grima-Pettenati, J.; Goffner, D. *Trends Plant Sci.* **2003**, *8*, 576.
27. Liu, C. H.; Xiao, C. B.; Liang, H. *J. Appl. Polym. Sci.* **2005**, *95*, 1405.
28. Canetti, M.; Bertini, F.; De Chirico, A.; Audisio, G. *Polym. Degrad. Stabil.* **2006**, *91*, 494.
29. Kai, W. H.; He, Y.; Asakawa, N.; Inoue, Y. *J. Appl. Polym. Sci.* **2004**, *94*, 2466.
30. Pérez, J.; Munoz-Dorado, J.; de la Rubia, T.; Martinez, J. *Int. Microbiology* **2002**, *5*, 53.
31. Bugnicourt, E.; Cinelli, P.; Lazzeri, A.; Alvarez, V. *eXPRESS Polym. Lett.* **2014**, *8*, 791.
32. Clarizio, S. C.; Tatara, R. A. *J. Polym. Environ.* **2012**, *20*, 638.
33. Marcovich, N. E.; Reboredo, M. M.; Kenny, J.; Aranguren, M. I. *Rheol. Acta* **2004**, *43*, 293.
34. Madbouly, S. A.; Schrader, J. A.; Srinivasan, G.; Liu, K. W.; McCabe, K. G.; Grewell, D.; Graves, W. R.; Kessler, M. R. *Green Chem.* **2014**, *16*, 1911.
35. Lu, H.; Madbouly, S. A.; Schrader, J. A.; Kessler, M. R.; Grewelle, D.; Graves, W. R. *RSC Adv.* **2014**, *4*, 39802.
36. Madbouly, S. A.; Otaigbe, J. U.; Ougizawa, T. *Macromol. Chem. Phys.* **2006**, *207*, 1233.
37. Canetti, M.; Bertini, F. *Compos. Sci. Technol.* **2007**, *67*, 3151.
38. Nitz, H.; Semke, H.; Mulhaupt, R. *Macromol. Mater. Eng.* **2001**, *286*, 737.
39. Hablot, E.; Matadi, R.; Ahzi, S.; Averous, L. *Compos. Sci. Technol.* **2010**, *70*, 504.
40. Grote, K. H.; Antonsson, E. K. Springer handbook of mechanical engineering (Vol. 10); Springer Science & Business Media, **2009**; p 211.
41. Maier, C.; Calafut, T. Polypropylene: The Definitive User's Guide and Databook, William Andrew Inc.: Norwich, NY, **2008**; p 113.